ESTEEM Academic Journal
Vol. 19, September 2023, 51-62

Characteristics of H_2S at Low Adsorption Temperature using Nitrogen-enhanced Carbon Modified with Ni Nanoparticles

Norfazilah Abdullah[1] and Norhusna Mohamad Nor[2]
[1,2]*Chemical Engineering Studies, Universiti Teknologi MARA, Cawangan Pulau Pinang, Permatang Pauh Campus, 13500 Pulau Pinang, Malaysia*
[2]*Waste Management and Resource Recovery (WeResCue) Group, Chemical Engineering Studies, Universiti Teknologi MARA, Cawangan Pulau Pinang, Permatang Pauh Campus, 13500 Pulau Pinang, Malaysia*
**corresponding author: [2]norhusna8711@uitm.edu.my*

ARTICLE HISTORY

Received
20 January 2023

Accepted
15 August 2023

Available online
29 September 2023

ABSTRACT

The main objective of this research is to investigate the adsorption characteristics of palm shell activated carbon (PSAC) adsorbent impregnated with nickel nanoparticles (Ni nps) and urea (Ni-N-PSAC) towards hydrogen sulfide (H_2S) gas removal at low adsorption temperature (30°C). The impregnation of Ni nps is expected to enhance the oxygen functional groups onto the adsorbent's structure, whereas the impregnation of urea will contribute to tailoring the nitrogen functional groups. It is expected that the Ni-N-PSAC adsorbent will exhibit heightened efficiency in removing H_2S at low adsorption temperature conditions. The H_2S adsorption was tested at various operating conditions such as different feed flowrate (100 – 250 ml/min), relative humidity, %RH (0 – 80 %RH) and H_2S feed concentrations (1000 – 4000 ppm). The adsorption characteristics of H_2S onto Ni-N-PSAC adsorbent were analyzed using adsorption isotherms and kinetics studies. The highest H_2S adsorption capacity calculated was 114.66 mg H_2S/g Ni-N-PSAC, where the adsorption parameters were at 100 ml/min, 30°C, 1000 ppm H_2S and 40 %RH. The removal of H_2S at low temperatures using Ni-N-PSAC showed that Temkin isotherm represents the best adsorption characteristics with R^2 = 0.9653. The kinetic study suggests that Pseudo second-order yields the most favourable result (R^2 = 0.9967). The outcome of this work is expected to provide new knowledge on the adsorption characteristics of H_2S using Ni-N-PSAC adsorbent at low adsorption temperature (30°C).

Keywords: *activated carbon; low adsorption temperature; H_2S removal; nickel nanoparticles; nitrogen functional groups*

1. INTRODUCTION

According to the World Health Organization (WHO) data, air pollution kills an estimated seven million people globally yearly. Air pollution containing hydrogen sulphide (H_2S) creates a major hazard to humans and the environment. The gas is often present in natural gas, biogas, landfills, coal gasification, wastewater treatment plants, and other refining industries [1]. H_2S should not be emitted directly into the atmosphere because it has a very unpleasant smell and is corrosive to metal equipment, especially machines and pipelines in industries [2], [3]. Exposure of this gas to humans at as low as 0.0047 ppm can lead to nausea, loss of appetite and other negative health effects [4]. The oxidation of H_2S into SO_2 in the atmosphere contributes

p-ISSN 1675-7939; e-ISSN 2289-4934

to the formation of acid rain and ozone layer depletion [5]. Therefore, it is extremely necessary to remove H_2S prior to utilization.

Such situations have led to the development of promising technologies towards H_2S removal. These technologies include biological treatment, chemical absorption and adsorption using mesoporous materials [6]. Biological treatment for H_2S removal reduces chemical, operating and energy costs. However, it requires a higher capital cost than the dry-based process [7]. Chemical absorption was proven to achieve 99.99% of sulphur removal efficiencies or higher, but this method contributes to plugging and foaming problems. Among the array of available technologies, adsorption is the most prevalent method for H_2S removal [9]. It is economical and feasible due to the availability of selective low-cost adsorbents such as activated carbon (AC), zeolites, naturally occurring materials and synthesized materials [8].

Amongst the adsorbent, AC is a widely used adsorbent for H_2S removal [10]. This is due to its unique characteristics, which are highly porous, high activity, long lasting [2], high surface area, favourable pore size [11] and high removal capacity compared to zeolite, metal-organic, porous silica, and clay incandescent [6]. Previous studies showed that the utilization of AC is efficient for treating H_2S gas below 10000 ppm [12]. AC can be derived from lignocellulosic biomass such as coconut shells, sawdust, agricultural waste, agricultural by-products [10], palm shells and corncobs [12]. Among all, palm shell is proposed to be used as a prospective starting material for AC due to its relatively high fixed carbon content, which is approximately 18% w/w, low ash content of less than 0.1% w/w and the presence of naturally existing porous structures [13]. Nevertheless, the mixture of metal oxides and porous carbon has a low breakthrough time, particularly at lower temperatures. Hence, it is anticipated to investigate the employment of metal oxide nanoparticles such as nickel (Ni) nanoparticles in improving the H_2S adsorption capacity via oxygen vacancies available in the carbon porous structure [14]. In addition, nitrogen functional group hold equal significance as oxygen functional groups in improving the AC's surface characteristics [15].

The equilibrium relationship between the distribution of H_2S onto the adsorbent's surface and in the bulk gas stream can be described and verified using various isotherm models [16]. Numerous isotherm models, including the Dubinin-Radushkevich, Temkin, Freundlich, and Langmuir have been developed and applied to analyze gas adsorption characteristics [17]. The adsorption process characteristics depend on the adsorption equilibrium data, which can be verified using isotherm's empirical models via linear regression to fit the experimental data. Adsorption kinetics describes the rate at which a given amount of adsorbate is adsorbed onto the surface or porous structure of a given amount of adsorbent [18]. Due to the fact that the adsorption process is time-dependent, kinetic study is crucial to establish the adsorption rate, which is necessary for the adsorption system's process design.

Recently, research efforts on H_2S removal using impregnation of metal oxides onto AC adsorbent require high adsorption temperature to achieve good adsorption performance. Hence, in this work, the team utilized our modified AC adsorbent reported earlier to remove H_2S at low adsorption temperatures [14]. The main purpose of this paper is to understand the characteristics of H_2S adsorbed onto the adsorbent at low adsorption temperature (30°C) through the application of adsorption isotherms and kinetic models.

p-ISSN 1675-7939; e-ISSN 2289-4934

2. MATERIALS AND METHODS

The overall process flow chart for this research work is presented in Figure 1.

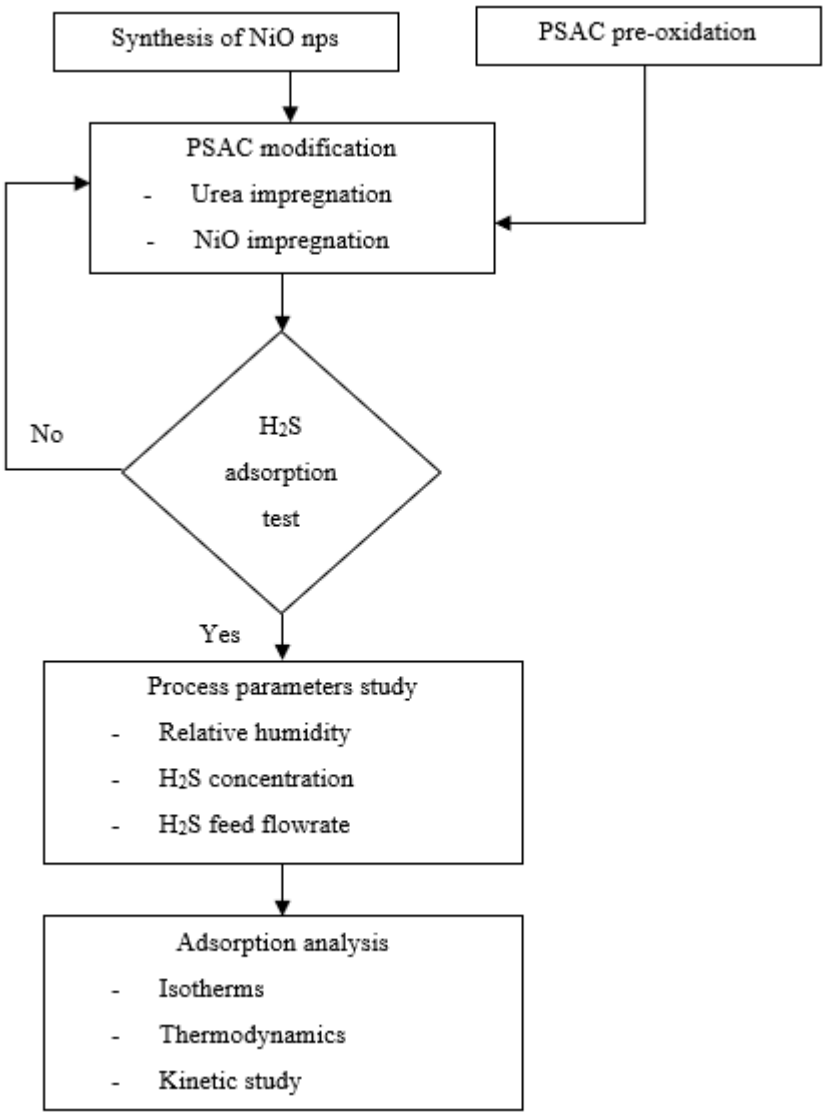

Figure 1: Overall process flow chart for this research work

2.1 Material and Chemicals

A commercial granular palm shell activated carbon (PSAC) was purchased from Nikom Carbon Technology Sdn. Bhd. In the nickel oxide nanoparticles (NiO nps) synthesis step, nickel (II) nitrate hexahydrate (Merck, ≥99.999%), ethanol (Merck, 96%) and polyvinylpyrrolidone (PVP) were used. In the urea impregnation step, nitric acid (HNO_3) (Merck, 50%), urea (Merck, 99%) and ethanol (Merck, 96%) were used. In the H_2S adsorption test, 99.99% N_2 and 1% H_2S in N_2, supplied by Linde Malaysia Sdn. Bhd. were used. The modified PSAC adsorbents were denoted as Ni-N-PSAC.

p-ISSN 1675-7939; e-ISSN 2289-4934

2.2 Synthesis of NiO nps

The NiO nps were synthesized using the alkaline precipitation method with some modifications [19]. A 4.65 g of $Ni(NO)_3.6H_2O$ powder was dissolved in a 20 mL mixture of distilled water and ethanol (1:1 v/v). The solution was added into a 1 g of PVP that dissolved in another 20 mL mixture of distilled water and ethanol (1:1). The PVP in the solution acted as a non-ionic surfactant to regulate nucleation and crystal growth, reduced surface tension and stabilized metal nanoparticles [20]. Next, 5 mL of 6.5 M NH_4OH was added dropwise to the reaction mixture with continuous stirring at 300 rpm. The resultant mixture was then sonicated to 55 °C using an ultrasonic cleaner bath (Model: GT Sonic QTD series) for 15 minutes. The mixture was let to rest for 15 minutes and sonicated again to 65 °C for another 15 minutes for the activation of nano metal hydroxide. After the sonication, it was allowed to cool to room temperature and was centrifuged using a table-top centrifuge (Model: Kubota 4200) at 6000 rpm for 10 minutes. The nanoprecipitate was washed and centrifuged using distilled water and ethanol (1:1) until the desired pH was around ~7. The green nanoprecipitate (NiO nps) was finally dried in an oven at 50 °C for 24 hours.

2.3 Urea Impregnation onto PSAC

This method was implied to introduce nitrogen containing (N-) functional groups. A 30 g of pre-oxidized PSAC was mixed with 20 g of urea in 100 mL of ethanol. The mixture was stirred at room temperature for 5 hours. Then the mixture was boiled to 78.5 °C, evaporating the alcohol and the PSAC was dried overnight at 110 °C. After modifications, the adsorbents, denoted as N-PSAC, were washed with boiling water to remove any excess urea [15].

2.4 Impregnation of NiO nps onto PSAC

A 25 mL of NiO nps solution of 6wt% metal amount was added to 2.50 g of N-PSAC in a conical flask each. The mixture was impregnated for 1.5 hours using an orbital shaker. After the impregnation, the PSAC was filtered and dried in an oven at 80°C for 24 hours. The dried impregnated PSAC was then subjected to calcination in a quartz tubular furnace at 400°C for 3 hours under the flow of N_2 at 50 mL/min. The N-PSAC after treatment is referred to as Ni-N-PSAC.

2.5 Continuous Fixed-bed H_2S Adsorption

The performance of the Ni-N-PSAC adsorbent was tested in a custom-designed H_2S adsorption rig. A 1 g Ni-N-PSAC adsorbent was weighed and placed in the middle of a stainless-steel column with 250 mm length and 9.525 mm diameter, supported with 0.3 g borosilicate glass wool. A simulated gas containing 1% H_2S in N_2 (1000 ppm, 2000 ppm, 3000 ppm and 4000 ppm) was passed through the column at a flowrate of 100 mL/min, 150 mL/min, 200 mL/min and 250 mL/min at low adsorption temperature. The composition of simulated gas was adjusted by controlling the flowrate of gases using Dwyer mass flow controllers. N_2 was passed through a humidification system to give approximately 0%, 40%, 60% and 80% relative humidity to the gases inlet stream. H_2S was not passed through the humidification system as it is soluble in water. The inlet and outlet of concentration of H_2S were monitored using MRU Optima7 portable biogas analyzer via an electrochemical sensor calibrated for the 0–4000 ppm range of H_2S concentration. The outlet concentration of H_2S was recorded continuously for every minute, and the adsorption test was stopped when the adsorbent became saturated. The

p-ISSN 1675-7939; e-ISSN 2289-4934

experiment was done in a fume hood, and the workspace of the H_2S rig was equipped with H_2S sensor as a safety precaution to detect H_2S leakage while carrying out the experiment. The adsorption capacity of the adsorbents was calculated as in Equation 1.

$$q = \frac{Q_f t_t y_f}{m_c} \tag{1}$$

where q is the adsorption capacity of fresh adsorbent (mg/g), Q_f is the volumetric feed flowrate (mL/min), y_f is the mole fraction of the adsorbate, t_t is the total time (min), and m_c is the mass of adsorbent (g).

2.6 Adsorption Isotherms

Adsorption isotherms were performed at a low operating temperature of 30°C. In order to investigate the adsorption equilibrium of H_2S, the H_2S feed concentration was varied from 1000 to 4000 ppm. This study applied four adsorption isotherms, namely Langmuir, Freundlich, Temkin isotherm and Dubinin-Radushkiev, to investigate the H_2S adsorption properties. The applicability and suitability of the isotherm equation to the equilibrium data were compared by judging the values of the correlation coefficients, R^2. The higher the R^2 value (R^2 =1), the better the fit is. Linearization of Langmuir, Freundlich, Temkin isotherm and Dubinin-Radushkiev isotherm models are shown in Equations 2, Equations 3, Equations 4, and Equations 5, respectively.

$$\frac{C_e}{Q_e} = \frac{1}{Q_m} C_e + \frac{1}{K_L Q_m} \tag{2}$$

$$lnQ_e = lna_F + b_F \, lnC_e \tag{3}$$

$$Q_e = \frac{R_T}{b_T} lnC_e + \frac{R_T}{b_T} lnA_T \tag{4}$$

$$lnQ_e = lnQ_d - K_{ad}\varepsilon^2 \tag{5}$$

where K_L and Q_m are the Langmuir isotherm constant related to the binding energy and monolayer adsorption capacity, a_F and b_F are Freundlich constant in which b_F is a measure of the surface heterogeneity, b_T and A_T are Temkin constants related to the heat of adsorption, and Q_d is the maximum adsorption capacity; k_{ad} is a Dubinin-Radushkiev constant related to the mean free energy of adsorption; ε is the Polanyi potential, respectively.

2.7 Adsorption Kinetics

In the kinetic study, H_2S adsorption was carried out under the condition of a low operating temperature of 30°C. In order for kinetic to describe the H_2S removal by using Ni-N-PSAC, two kinetic models, namely pseudo-first-order, and pseudo-second-order, were applied. Both models were linearized and fitted with the experimental data to study the kinetic parameters. The linearized equations for the pseudo-first and second-order models are outlined in Equation 6 and Equation 7, respectively.

p-ISSN 1675-7939; e-ISSN 2289-4934

$$ln(Q_e - Q_t) = -k_1 t + ln\ Q_e \quad (6)$$

$$\frac{t}{Q_t} = \frac{1}{k_2 Q_e^2} + \frac{t}{Q_e} \quad (7)$$

where Q_t is the adsorption capacity at time t, k_1 is the pseudo-first order rate constant, and k_2 is the pseudo-second order rate constant, respectively.

3. RESULTS AND DISCUSSION

3.1 Effect of H_2S Adsorption Operating Parameters

The synthesized Ni-N-PSAC adsorbent was tested under various H_2S adsorption parameters, which are relative humidity, gas feed flow rate, and feed concentration of H_2S. These parameters are essential in the adsorption process optimization, while understanding the H_2S adsorption behaviour to achieve efficient removal of H_2S from various gas streams/conditions. Figure 2 shows H_2S breakthrough curves at different adsorption parameters. Overall, H_2S was observed at the outlet within 2-3 minutes of operations. Subsequently, the H_2S concentration gradually increased until it reached equilibrium when the outlet concentration (C_i) was equal to the inlet concentration (C_o). The breakthrough time and breakthrough capacity values were calculated once C_i/C_o = 0.05 (5%). Table 1 outlines the adsorption capacity of H_2S using Ni-N-PSAC adsorbent at different adsorption parameters.

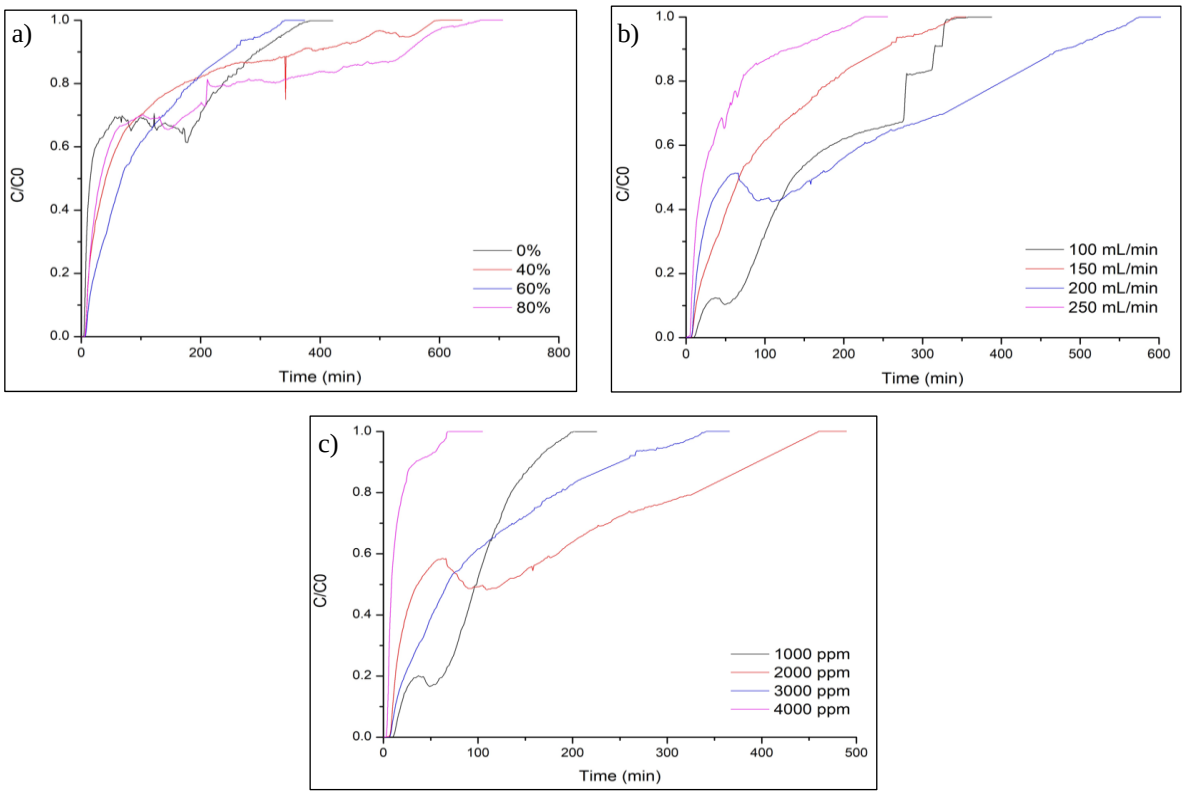

Figure 2: H_2S Breakthrough curves using Ni-N-PSAC adsorbent at different adsorption parameters a) relative humidity, b) gas feed flow rate, and c) initial H_2S concentrations.

p-ISSN 1675-7939; e-ISSN 2289-4934

Table 1: H_2S breakthrough and adsorption capacity of Ni-N-PSAC adsorbent at different adsorption parameters.

Adsorption parameter		Breakthrough time (min)	Breakthrough capacity (mg H_2S/g PSAC)	Total adsorption capacity (mg H_2S/g PSAC)
Relative humidity (%)	0	5.32	3.58	65.08
	40	7.96	5.35	74.44
	60	9.73	6.54	89.32
	80	8.17	5.49	96.44
Gas feed flow rate (mL/min)	100	16.61	11.16	114.66
	150	9.73	6.54	69.32
	200	9.70	6.52	130.99
	250	5.72	3.84	31.08
Initial H_2S concentration (ppm)	1000	16.62	11.17	92.18
	2000	8.60	5.78	71.70
	3000	9.73	6.54	69.32
	4000	4.06	2.73	10.40

The effect of water vapor on H_2S removal was investigated with different relative humidity (RH). From Table 1, it was observed that the adsorption capacity of H_2S increased when water vapor was introduced to the system. When water vapor was increased from 0 to 60%, the breakthrough capacity increased from 3.58 to 6.54 mg H_2S/g PSAC. However, when water vapor increased to 80%, the breakthrough capacity dropped to 5.49 mg H_2S/g PSAC. The same trend was observed for the H_2S total adsorption capacity. According to Sumathi et al., higher RH would enhance the dissociation of H_2S into HS^- and, in most cases, the dissociation step is the rate-limiting step in the adsorption process [21]. The competition between H_2S and water molecules for the active sites of the adsorbent was detrimental to H_2S removal. Furthermore, higher moisture content was discovered to deactivate the metal species embedded in the adsorbent and slow the reaction rate [21]. Nevertheless, sufficient amount of moisture content presence could enhance the H_2S adsorption capacity remarkably. This has been reported by Cimino et al. (2020), where 50% of RH introduced increased the H_2S total adsorption capacity up to 118 mg H_2S/g adsorbent [7].

It is clear that a higher adsorption capacity results from a lower gas feed flow rate. The H_2S breakthrough capacity drastically dropped from 11.16 to 3.84 mg H_2S/g PSAC when the gas feed flow rate was raised from 100 to 250 mL/min. This is because more H_2S molecules could be adsorbed when the flowrate was lower due to the gas stream containing H_2S had longer contact time with the adsorbent [22]. In contrast, increasing the gas feed flow rate will affect the mass transfer zone within the active site of the adsorbent if the H_2S molecules move rapidly. Therefore, AC took a longer time to adsorb all H_2S molecules from the stream until it reached a breakthrough, contributing to a higher adsorption capacity [22].

It can be observed that higher initial H_2S concentration contributed to lower H_2S adsorption capacity. The highest H_2S adsorption capacity was obtained when 1000 ppm of influent H_2S with 11.17 mg H_2S/ g PSAC. The lowest adsorption capacity was obtained at 4000 ppm with 2.73 mg H_2S/g PSAC. According to Choo et al. (2013), this outcome differed from the conventional research using batch experiments, as in this study, dynamic adsorption was implied [22]. The team found that in dynamic adsorption, the effect of driving force and mass transfer flux is minimal [22]. Furthermore, it is constrained by the rate of molecular diffusion into deeper pores as well as the adsorption process. When the influent H_2S concentration was lower, the impregnated activated carbon could absorb all the H_2S in the gas stream [22].

p-ISSN 1675-7939; e-ISSN 2289-4934

3.2 H_2S Adsorption Isotherms

Adsorption isotherm is an empirical relationship for predicting the quantity of solute that can be adsorbed by activated carbon. Figure 3 shows the H_2S adsorption isotherms plotted using Langmuir, Freundlich, Temkin and Dubinin-Radushkiev isotherm models for Ni-N-PSAC towards H_2S removal. To facilitate calculation, the H_2S concentration in ppm was converted to mg/L, and the adsorption capacity at various concentrations of H_2S was recorded in mg/g. All isotherms were fitted accordingly with the experimental data using the linear regression method. Based on the results, the equilibrium adsorption capacity of H_2S removal by Ni-N-PSAC adsorbent fitted well with Temkin isotherm as R^2 is closer to 1. However, the rest of the isotherm models did not fit well with the experimental data.

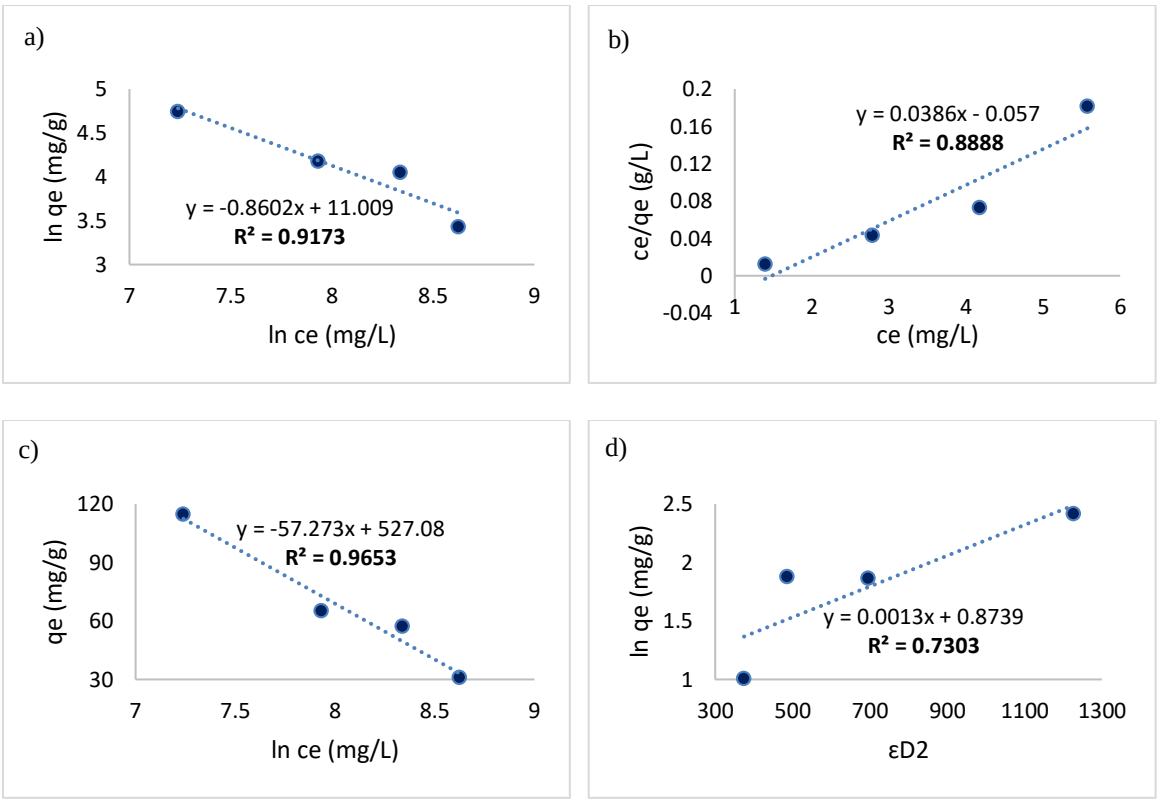

Figure 3: H_2S adsorption isotherms by using Ni-N-PSAC adsorbent at low adsorption temperature a) Freundlich Isotherm, b) Langmuir isotherm, c) Temkin isotherm, and d) Dubinin-Radushkiev isotherms.

Temkin isotherm model contains a factor of some indirect interactions between adsorbate and adsorbent on adsorption isotherm. Due to these interactions, the heat of adsorption of all molecules in the layer would decrease linearly with the increase in coverage of the adsorbent surface [23]. The adsorption mechanism by Temkin isotherm is characterized by a uniform distribution of binding energies. Temkin isotherm was derived under the assumption that the heat of adsorption decreases linearly as opposed to logarithmically. Furthermore, this model is applicable exclusively to chemical adsorption and has homogeneous binding energy [24]. This could imply that a chemical adsorption process was engaged in the H_2S adsorption employing the Ni-N-PSAC adsorbent. Isotherm parameters calculated for this work were summarized in Table 2 accordingly.

p-ISSN 1675-7939; e-ISSN 2289-4934

Table 2: Isotherms parameters of this study.

Adsorbent	Operating Conditions	Isotherm parameters	R^2
Nitrogen enhanced palm shell activated carbon with nickel nanostructured	H_2S concentration =1000 ppm Adsorption temperature = 30˚C Gas feed flow rate = 100 mL/min Relative humidity, %RH = 40% Ni-N-PSAC adsorbent = 0.3 g	**Freundlich** a_F=0.8602 b_F=11.009	0.9173
		Langmuir Q_m=25.91 K_L=0.677	0.8888
		Temkin B=57.273 K_T=1.0074 × 10^{-4}	0.9653
		Dubinin-Radushevich k_{DR}=0.0013	0.7303

3.3 Kinetic Studies of H_2S Adsorption

The adsorption kinetic study is significant in evaluating the performance of adsorbents and their mechanisms, especially the performance of sorbate-sorbent interaction in a fixed bed system [25]. Figure 4 shows the pseudo-first-order and pseudo-second-order kinetic models for H_2S adsorption using Ni-N-PSAC adsorbent at a low adsorption temperature (30°C). To study the kinetic parameters, the breakthrough curve data was redrawn using linearized pseudo-first-order (Eq. 6) and pseudo-second-order (Eq. 7) kinetic equations. Due to the low R^2 values, it was determined that the pseudo-first-order kinetic equation did not match the experimental data; hence, the data was omitted. The R^2 obtained from the pseudo-first-order kinetic model was found to be 0.6811, which was lower than that of the pseudo-second-order kinetic model (R^2 = 0.9967). This indicates that pseudo-second-order fitted well with the experimental data.

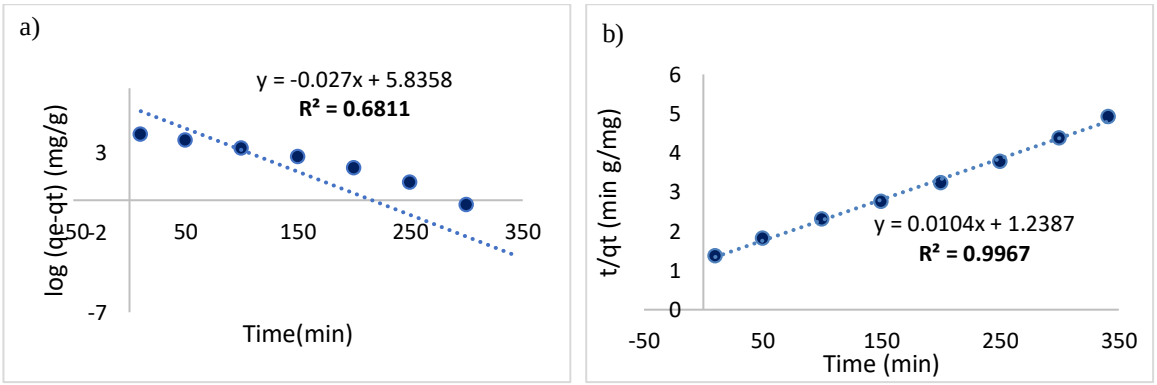

Figure 4: H_2S adsorption kinetics by using Ni-N-PSAC adsorbent at low adsorption temperature a) Pseudo first-order and b) Pseudo second-order models.

The pseudo-second-order model regards chemisorption as the rate-limiting mechanism of the process, in contrast to the pseudo-first-order model, which posits that physisorption restricts the adsorption rate of the particles onto the adsorbent [25]. In the pseudo-second-order kinetic model, chemisorption is the rate-limiting step, which indicates that the H_2S diffusions onto the Ni-N-PSAC adsorbent were based on chemical interactions [23]. This finding is supported by the characteristics of the Temkin adsorption isotherm, where the H_2S adsorption onto the adsorbent is solely dependent on chemical adsorption with homogeneous binding energy. The parameters for the pseudo-second-order kinetic equation obtained were tabulated in Table 3.

p-ISSN 1675-7939; e-ISSN 2289-4934

Table 3: Calculation for pseudo second order kinetic model.

Temperature (℃)	Slope	Intercept	R^2	Q_e	K_2
30	0.0104	1.2387	0.9967	96.15	0.000087

4. CONCLUSIONS

In this study, the characteristics of H_2S adsorption using Ni-N-PSAC adsorbent were evaluated accordingly. The analysis revealed that increased RH values will increase the H_2S adsorption capacity, while a low gas feed flow rate contributes to higher H_2S adsorption capacity. Similar to gas feed flowrate, decreasing the H_2S inlet concentration will provide higher H_2S adsorption capacity. From this work, the best adsorption parameters were found to be 40% of RH, 100 mL/min gas feed flowrate and 1000 ppm of H_2S inlet concentration with a total H_2S adsorption capacity of 114.66 mg/g. The results indicated that Ni-N-PSAC adsorbent could promote and enhance the removal of H_2S via chemisorption interaction, which is best fitted to Temkin adsorption isotherm and pseudo-second-order models, with R^2 = 0.9653 and R^2 = 0.9967, respectively.

ACKNOWLEDGEMENT

The authors would like to acknowledge the financial assistance funded by Fundamental Research Grant Scheme (600-IRMI/FRGS 5/3 (022/2019)) and the facilities provided by Universiti Teknologi MARA Cawangan Pulau Pinang in the completion of this work.

CONFLICT OF INTEREST

The authors declare no conflicts of interest in publishing this paper. Authors have the option to disclose any potential conflicts of interest.

REFERENCES

[1] A. G. Georgiadis, N. D. Charisiou, and M. A. Goula, "Removal of hydrogen sulfide from various industrial gases: A review of the most promising adsorbing materials" *Catalysts*, vol. 10, no. 5, 2020.

[2] R. Sitthikhankaew, S. Predapitakkun, R. Kiattikomol, S. Pumhiran, S. Assabumrungrat, and N. Laosiripojana, "Comparative study of hydrogen sulfide adsorption by using alkaline impregnated activated carbons for hot fuel gas purification" *Energy Procedia*, vol. 9, pp. 15–24, 2011.

[3] G. Imanzadeh, H. Basharnavaz, A. Habibi-yangjeh, and S. H. Kamali, "Adsorption behavior of H_2S on P – doped , V/P , Nb P , and Ta/P – codoped graphitic carbon nitride : A first-principles investigation" *Mater. Chem. Phys.*, vol. 252, no. January, p. 123117, 2020.

[4] J. Guo *et al.*, "Adsorption of hydrogen sulphide (H_2S) by activated carbons derived from oil-palm shell" *Carbon N. Y.*, vol. 45, no. 2, pp. 330–336, 2007.

[5] N. Kumar, J. Bae, S. Kim, and K. Soo, "Chemosphere Fabrication of Zn-MOF / ZnO nanocomposites for room temperature H_2S removal : Adsorption , regeneration , and mechanism" *Chemosphere*, vol. 274, p. 129789, 2021.

[6] N. N. Zulkefli *et al.*, "Removal of hydrogen sulfide from a biogas mimic by using impregnated activated carbon adsorbent" *PLoS One*, vol. 14, no. 2, 2019.

p-ISSN 1675-7939; e-ISSN 2289-4934

[7] S. Cimino, L. Lisi, A. Erto, F.A. Deorsola, G. de Falco, F. Montagnaro, M. Balsamo, "Role of H_2O and O_2 during the reactive adsorption of H_2S on CuO-ZnO/activated carbon at low temperature" *Microporous Mesoporous Mater.*, vol. 295, no. 15, pp 109949, 2020.

[8] A. H. Abdullah, R. Mat, S. Somderam, A. Shah, A. Aziz, and A. Mohamed, "Hydrogen Sulfide Adsorption by Zinc Oxide-Impregnated Zeolite (Synthesized from Malaysian Kaolin) for Biogas Desulfurizatio," *J. Ind. Eng. Chem.*, 2018.

[9] S. M. Abegunde, K. S. Idowu, O. M. Adejuwon, T. Adeyemi-Adejolu, "A review on the influence of chemical modification on the performance of adsorbents" *Resour. Environ. Sustain.*, vol. 1, pp. 100001, 2020.

[10] F. M. Marsin, W. A. W. Ibrahim, H. R. Nodeh,, Z. A. Sutirman, N. N. Ting, "Recent Advance in the Preparation of Oil Palm Waste-based Adsorbents for Removal of Environmental Pollutants - A Review," *Malaysian J. Anal. Sci.*, vol. 22. no. 2, pp. 175 - 184, 2018.

[11] N. Mohamad Nor, L. C. Lau, K. T. Lee, and A. R. Mohamed, "Synthesis of activated carbon from lignocellulosic biomass and its applications in air pollution control - A review" *J. Environ. Chem. Eng.*, vol. 1, no. 4, pp. 658–666, 2013.

[12] R. Sitthikhankaew, D. Chadwick, and S. Assabumrungrat, "Performance of Sodium-impregnated activated carbons towards low and high temperature H_2S adsorption" *Chem. Eng. Commun.*, no. October, pp. 37–41, 2014.

[13] A. R. Yacob, Z. A. Majid, R. Sari, and D. Dasril, "Comparison of various sources of high surface area carbon prepared by different types of activation" *Malaysian J. of Anal. Sci.*, vol. 12, no. 1, pp. 264–271, 2008.

[14] N. Abdullah, A. R. Mohamed, M. Z. Ramli, and N. M. Nor, "Influence of Surface Characteristics of Palm Shell Activated Carbon Modified with Nanostructured Nickel for Reactive Adsorption of Hydrogen Sulfide" *J. Appl. Sci. Eng.*, vol. 25, no. 3, pp. 505–512, 2022.

[15] N. M. Nor, L. L. Chung, and A. R. Mohamed, "Nitrogen Tailored Activated Carbon via Microwave Synthesis Method for High Removal of Hydrogen Sulfide" *Malaysian J. Fundam. Appl. Sci.*, vol. 17, no. 6, pp. 794–804, 2021.

[16] D. Papurello, M. Gandiglio, and A. Lanzini, "Experimental analysis and model validation on the performance of impregnated activated carbons for the removal of hydrogen sulfide (H_2S) from sewage biogas" *Processes*, vol. 7, no. 9, 2019.

[17] L. Chung Lau, "Adsorption Isotherm, Kinetic, Thermodynamic and Breakthrough Curve Models of H2S Removal Using CeO2/NaOH/PSAC," *Int. J. Petrochemical Sci. Eng.*, vol. 1, no. 2, pp. 36–44, 2016.

[18] D. Qarizada, N.M.R. Noraini, A.B. Alias, M. F. Fadil, H. Kambakhsh, "Equilibrium isotherm and adsorption kinetics model of hydrogen sulphide using xerogel derive from palm kernel shell biochar" *Int. J. Eng. Adv. Res.*, vol. 4, no. 4, pp. 16-33, 2022.

[19] I. W. Siriwardane *et al.*, "Synthesis and characterization of nano magnesium oxide impregnated granular activated carbon composite for H2S removal applications" *Mater. Des.*, vol. 136, pp. 127–136, Dec. 2017.

[20] S. M. Lam, M. W. Kee, and J. C. Sin, "Influence of PVP surfactant on the morphology and properties of ZnO micro/nanoflowers for dye mixtures and textile wastewater degradation" *Mater. Chem. Phys.*, vol. 212, pp. 35–43, 2018.

[21] L. Chung, N. Mohamad, K. Teong, and A. Rahman, "Journal of Environmental Chemical Engineering Hydrogen sul fi de removal using CeO2 / NaOH / PSAC : Effect of process conditions and regeneration study," *Biochem. Pharmacol.*, vol. 4, no. 3, pp. 3479–3483, 2016.

[22] H. Sun Choo, L. Chung Lau, A. Rahman Mohamed, and K. Teong Lee, "Hydrogen Sulfide Adsorption by Alkaline Impregnated Coconut Shell Activated Carbon" *J. Eng. Sci. Technol.*, vol. 8, no. 86, pp. 741–753, 2013.

[23] S. Wang, H. Nam, T. B. Gebreegziabher, and H. Nam, "Adsorption of acetic acid and hydrogen sulfide using NaOH impregnated activated carbon for indoor air purification" *Eng. Reports*, vol. 2, no. 1, pp. 1–22, 2020.

p-ISSN 1675-7939; e-ISSN 2289-4934

[24] M. Mukherjee *et al.*, "Ultrasonic assisted graphene oxide nanosheet for the removal of phenol containing solution" *Environ. Technol. Innov.*, Jan. 2017.
[25] È. Ersoy-meric, "Modeling of the isothermal sulphation reactions of natural sorbents" vol. 319, 1998.

p-ISSN 1675-7939; e-ISSN 2289-4934